Electrical Supplementary Information

Title: Rapid crystal growth of bimetallic PdPt nanocrystal with surface atomic Pt cluster decoration performs promising oxygen reduction activity

Authors: *Kuan-Wen Wang,[1] Zhuang, Yu,[2] Hu, Alice,[2] Yang-Yang Hsu,[3] Tian-Lin Chen,[3] Cheng-Yang Lin,[4] Chih-Wei Hu,[3] Ya-Tang Yang,[4] and Tsan-Yao Chen [3,5]**

Affiliations:

1. Institute of Materials Science and Engineering, National Central University, Taiwan.
2. Department of mechanical and biomedical engineering, City University of Hong Kong, Kowloon, HK
3. Department of Engineering and System Science, National Tsing Hua University, Hsinchu 30013, Taiwan. E-mail: chencaeser@gmail.com; TEL: +886-3-5715131#34271.
4. Department of Electrical Engineering & Institute of Electronic Engineering, National Tsing Hua University, Hsinchu 30013, Taiwan.
5. Institute of Nuclear Engineering and Science, National Tsing Hua University, Hsinchu 30013, Taiwan.

*To whom correspondence should be addressed:
Tsan-Yao Chen, E-mail: chencaeser@gmail.com, TEL: +886-3-5715131#34271.

1. Preparation of electrode for ORR activity test

The slurry sample for ORR experiment was made of 5.0 mg active carbon supported NC which mixes distilled water (14.0 ml), IPA (6.0 ml), and 5 wt% Nafion (0.1 ml). The mixture is stirred at 250 rpm for 30-min prior to an ultrasonication bath at 30^{o}C for 30-min. For preparing working electrode in the ORR sweeping experiment, the slurry (20.0 ul) was dropped and dried in top of a rotation graphite electrode (diameter = 5.0 mm). The linear sweep voltammetry (LSV) data was collected using a potentiostat (CH Instruments Model 600B) equipped with a three-electrode electrochemical system. This system consists of a standard electrode of Mercury oxide electrode (the voltage is calibrated by 0.098 V in alignment to that of RHE), a counter electrode of Pt metal wire, and a working electrode. The electrolyte is an aqueous solution of KOH (0.1M). The voltage scan rate is 5 mV s^{-1} for LSV and 50 mV s^{-1} for acceleration degradation test (ADT). In these electrochemical tests, the rotation speed of electrode is 1600 rpm. For reducing the complexity of discussions, the structural characterizations are conducted only on the control sample and NC with optimum electrochemical performances. The proposed structure to property correlations are clarified by comparing results of the electrochemical surface test before and after ADT.

2. TEM Characterization on experimental PdPt NPs

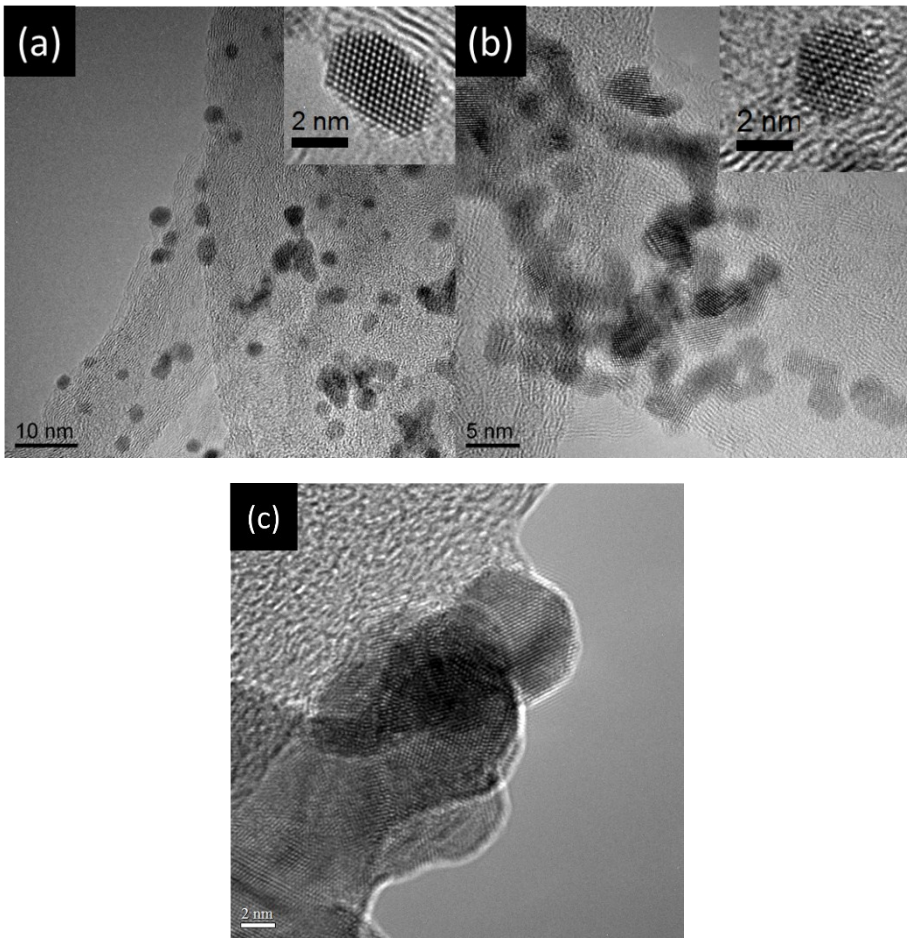

Figure S1 TEM images of Pt-s NP before (a) and after (b) ADT by 5000 cycles. Insets show the HRTEM atomic images of the samples. (c) HRTEM image of Pd-s NC.

TEM and atomic images of Pt-s before and after ADT by 5000 cycles are shown in **Figure S1**. As can be seen, Pt NP of Pt-s is well dispersed in CNT support (**Figure S1a**) with ordered atomic structure (**Figure S1a** inset). A preferential crystal growth is found at (111) facets with rocky (steps, terrace, and edges) surface in NPs. Atoms in those unstable defect sites will be restructured in high coordination structure region, therefore, resulting in the inter-particle aggregation (**Figure S1b**) and surface rounding (**Figure S1b** inset) in minimizing the surface free energy of NPs. **Figure S1c** shows HRTEM image of Pd-p NC. As clearly revealed, Pd NC is grown in isotropic shape with similar surface morphology in all facets.

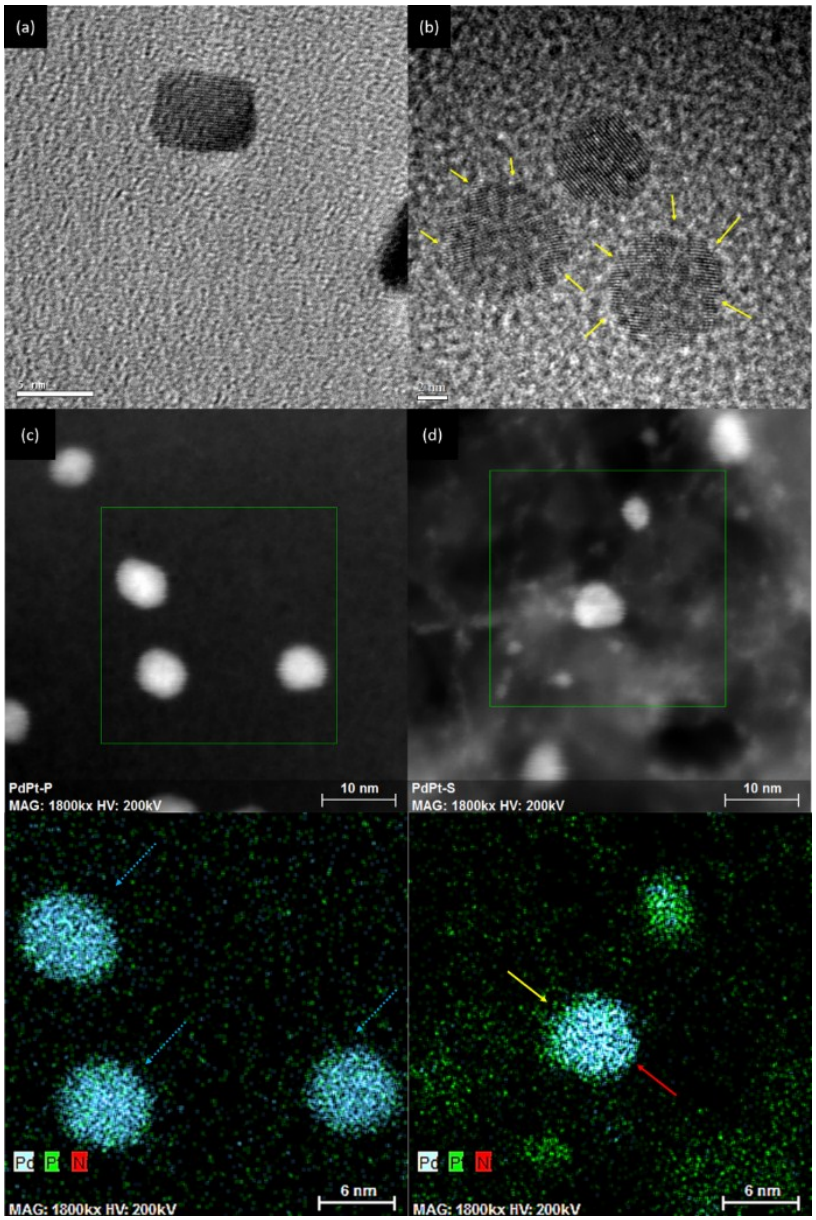

Figure S2 High resolution TEM images of (S2a) Pt and (S2b) Pd nanoparticles prepared by polyol reduction method. The reaction system controlled in a metal precursor concentration of 20 mM in a presence of 10 wt% PVP-40 polymer vs. reaction solvent (ethylene glycol). Dark field scanning transmission electron microscope (STEM) images of PdPt-p and PdPt-p with corresponding EDX maps are respectively compared in Figure S2c and S2d.

HRTEM images of PVP blended Pt, Pd NPs synthesized by the same metal content and stabilizer concentration in polyol reduction method and experimental PdPt-s, PdPt-p NPs. As shown (**Figure S2a**), Pt NPs tend to form rectangular shape with a preferential growth at (111) facet. It means a strong steric confinement at higher indexes facets in the presence of PVP ligands. On the other hand, rocky surface with (111) facets exposed

to different directions is found in Pd NP (**Figure S2b**). Such a high roughness surface (see yellow arrows) features the nature of multi-facets crystal growth due to the weak steric confinement by PVP chelation at Pd NPs. To confirm the element distribution of Pd and Pt atoms on experimental PdPt NPs, scanning transmission electron microscope (STEM) analysis is employed. As indicated by **dashed blue lines** in **Figure S2c**, Pd and Pt atoms are uniformly distributed in PdPt-p NP. Such a result consistent with the XRD analysis reveals the formation of homogeneous alloy. On the other hand, PdPt-s NP is formed by stacking Pt atoms in specific corner (see **yellow solid arrow**) at Pd NP body (see **red solid arrow**) surface.

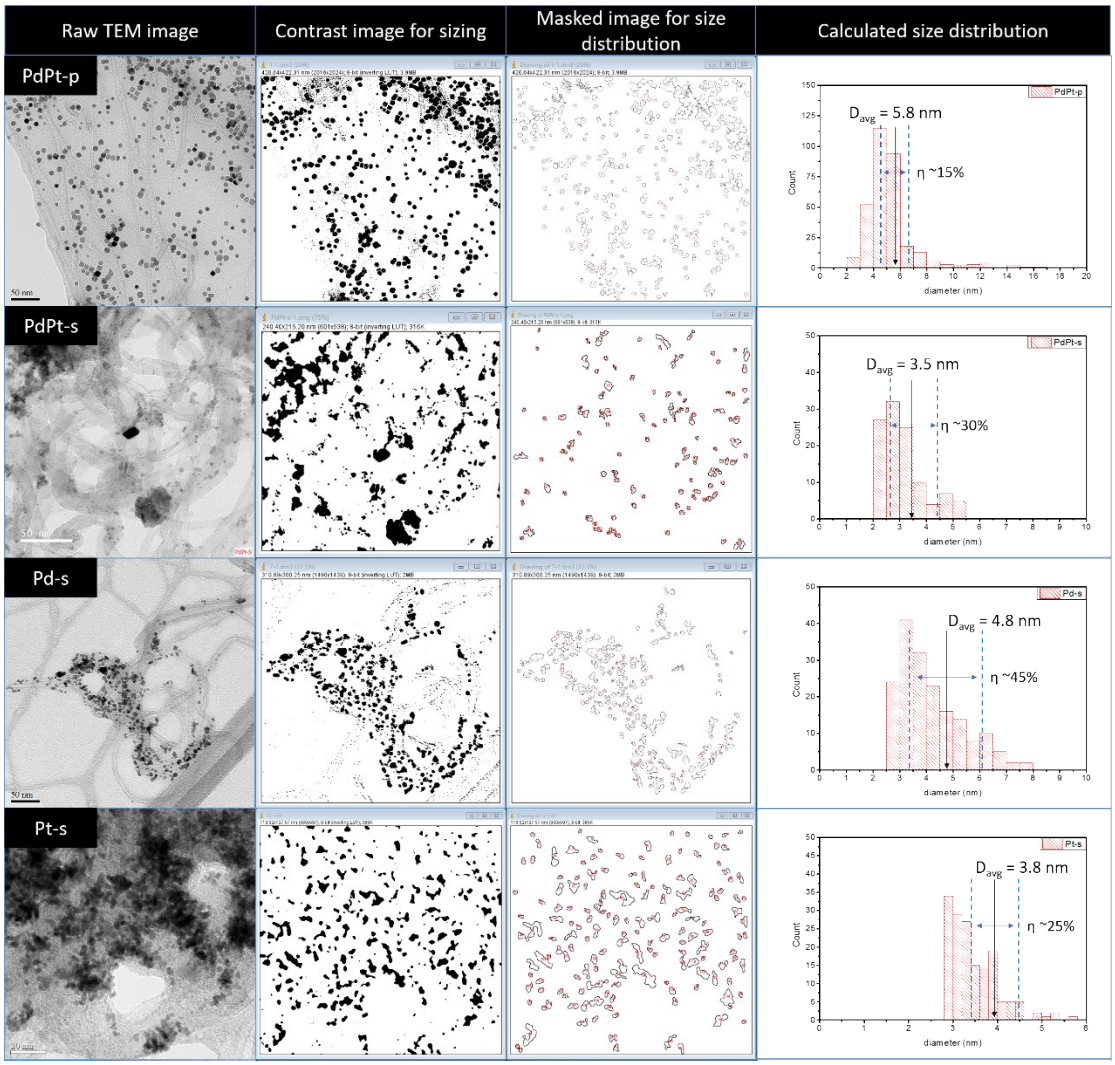

Figure S3 TEM images and size distribution of PdPt-p, PdPt-s, Pd-s, and Pd-s NPs.

Size distributions of experimental samples are estimated both by using TEM (**Figure S3**) and XRD analysis. As demonstrated, average particle size (D_{avg}) is determined to

be 5.8 nm for PdP-p, 3.5 nm for PdPt-s, 4.8 nm for Pd-s, and 3.8 nm for Pt-s. Among experimental NPs, PdPt-p gains the smallest particle size distribution (η +/- 15% vs. D_{avg}) and is reasonably explained by the steric confinement of crystal growth by polymer stabilizers at specific facets (110 in most cases). It is easy to understand that Pd-s gains the largest η owing to the higher atomic diffusion coefficient (D_{int} α Z, Z is atomic number) of Pd compared to that of Pt.

3. Geometrical structure calculation on PdPt NPs

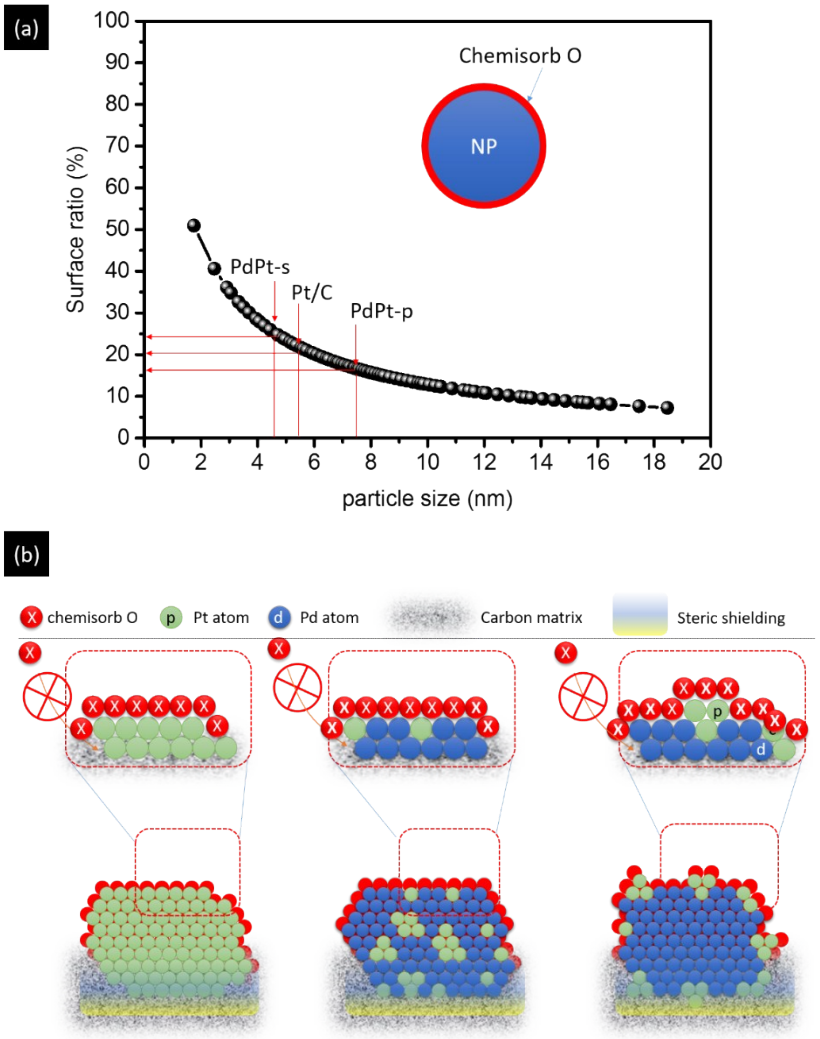

Figure S4 Geometrical correlation of NPs (a) changes of surface to bulk ratio of spherical NP with particle size without steric shielding of carbon and (b) schematic representation of chemisorb O in experimental NP surface. Carbon support form a steric shielding to suppress chemisorb O in NP surface at interface.

Comparison between surface to bulk ratio and extent of oxidation further reveals location of Pt atoms in NPs; where correlations of spherical nanoparticle can be estimated by geometry calculations and are discussed as simplified interpretations. As shown in **Figure S4a**, surface to bulk ratios (η) are 34.8% for PdPt-s (3.5 nm), 30.1% for Pt-s (3.8 nm), and 23.1% for PdPd-p (5.8 nm) with a known size. Considering that all PdPt NPs are grown in homogeneous alloy, the oxidation extent of Pt (determined by fitting corresponding XANES spectra using linear combination fitting method) should be determined to a similar value to their η (PdPt-p). In this event, a slightly lower Pt oxidation to η (also found in Pt-s) could be attributed to the protection of Pt from

oxidation by carbon support at interface (i.e., steric shielding effects of carbon contact to oxygen coverage in NP surface in **Figure S4b**). However, extent of Pt oxidation is determined to be 38.2% for PdPt-s. This value is far higher than that is expected in homogeneous alloy and can only be rationalized by exposing Pt clusters to NP surface (i.e., decoration of Pt atoms in NP surface).

4. Electrochemical analysis on PdPt NPs in ADT

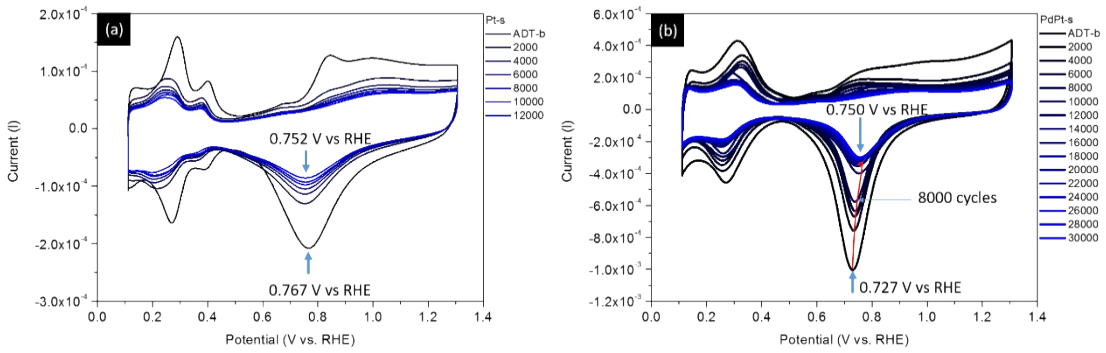

Figure S5 CV sweeping curves of (a) Pt-s and (b) PdPt-s NPs. Potential of oxygen adsorption peak of Pt-s progressively decreased from 0.767 V vs. RHE to 0.752 V vs. RHE with ADT till 12000 cycles. For PdPt-s, potential of oxygen adsorption peak increases by 0.023 V by ADT till 30000 cycles. Upon ADT, a fluctuation of peak potential at ~0.727 to 0.750 V vs. RHE (see red solid arrow) indicates the changes of chemisorption states for oxygen adsorption in PtPd-s surface.

5. XPS analysis on Pt-s, Pd-s, PdPt-s, and PdPt-p

According to **Table S1**, Pt/Pd ratios of PdPt-p and PdPt-s are 15/85 and 34.4/65.6, respectively. It is expectable to find that Pt atoms are prefer to locate in NC surface due to the experimental design with sequence control on metal reduction. For PdPt-s, Pt atoms are reduced by interacting with $NaBH_4$ after formation of Pd NC. In such an event, the surface ratio to bulk ratio is about 30 to 40 % for Pd NC with an average size around 8 – 10 nm. Our XPS results suggest that majority of Pt atoms are located in PdPt-s surface. On the other hand, Pt atoms tend to homogeneous distributed in core region of PdPt-p as consistently revealed by cross-referencing XPS and CO stripping results (**Figure S7**). Given that, a strong reduction agent ($NaBH_4$) with over dose is employed for growing PdPt-s, we believed that most of metal ions (which are easy growth Pd and Pt) were reduced in synthetic procedures. It means that the deviation on mass activity estimation in electrochemical results should properly refer to the realistic status of experimental samples.

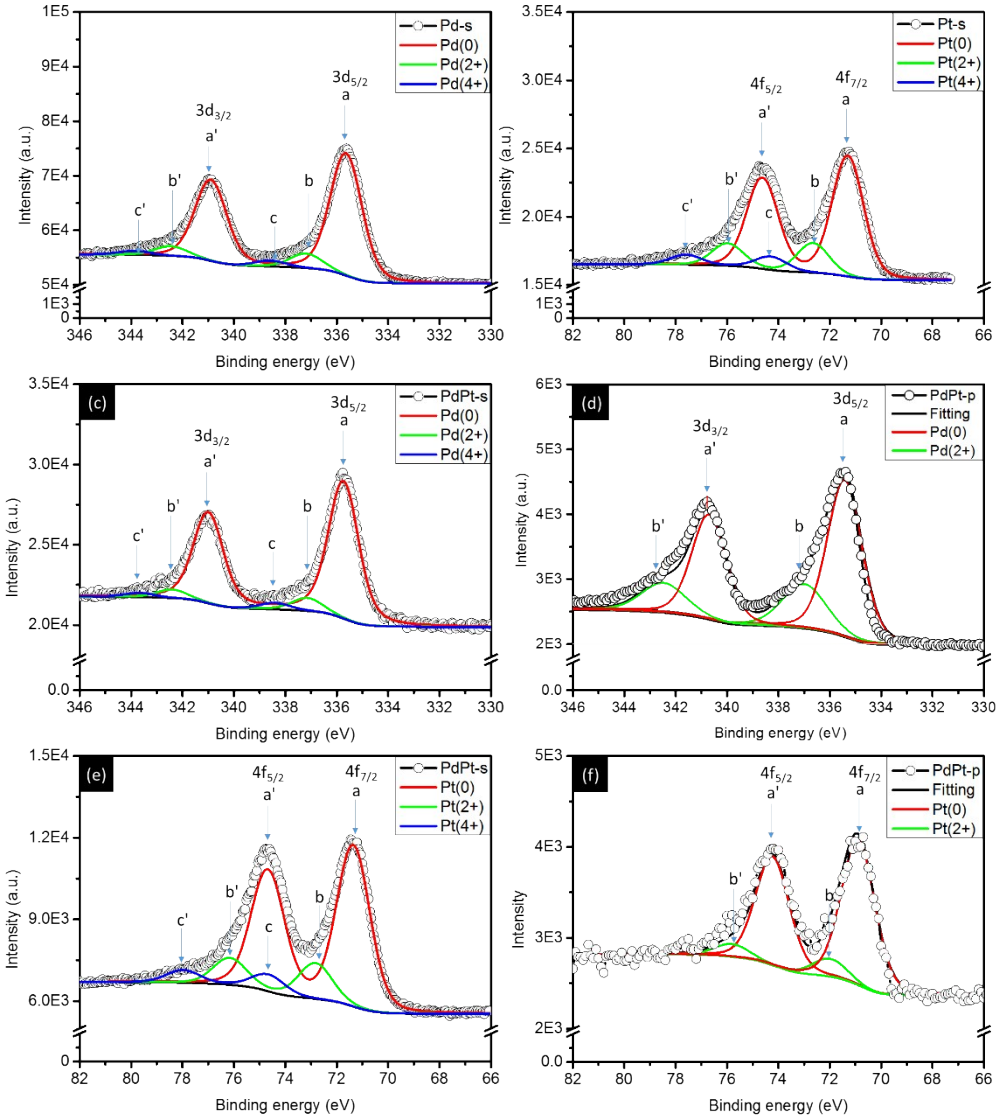

Figure S6 XPS spectra of experimental NCs at Pd 3d orbital for (a) Pd 3d of Pd-s, (b) Pt 4f of Pt-s, (c) Pd 3d of PdPt-s, (d) Pt 4f of PdPt-p, (e) Pd 3d of PdPt-s, and (f) Pt 4f of PdPt-p NCs.

Table S1 XPS fitting results of experimental NCs

	Pt chemical states			Pd chemical states			Composition (%)	
Sample	Pt0	Pt 2+	Pt 4+	Pd0	Pd 2+	Pd 4+	Pt	Pd
J.M.PtC	72.42	19.0	8.58	-	-	-	100	-
PdCNT	-	-	-	85.84	10.1	4.06	-	100
PtCNT	73.75	18.11	8.14	-	-	-	100	-
PdPt-s	75.37	16.7	7.92	87.68	8.29	4.04	34.4	65.6
PdPt-p	80.0	20.0		73.0	27.0		15.0	85.0

Table S1 (cont.) XPS fitting results of experimental NCs

	Binding energy (eV)					
Sample	Pt0	Pt 2+	Pt 4+	Pd0	Pd 2+	Pd 4+
J.M.PtC	71.36	72.51	74.06	-	-	-
PdCNT	-	-	-	335.6	337.2	338.6
PtCNT	71.29	72.65	74.27	-	-	-
PdPt-s	71.36	72.83	74.65	335.7	337.2	338.4
PdPt-p	70.91	72.05		335.5	337	

6. CO stripping analysis on Pt-s, Pd-s, PdPt-s, and PdPt-p NCs

ECSA of CO stripping area have been calculated and results are discussed in revised ESI. ECSA is valid for pure Pt catalysts, but very difficult to accurately quantify for any non-Pt surfaces. From conventional understandings, the H_{upd} method is the most accurate method for Pt. ECSA from CO stripping curve can adopt similar method. In this case, a value of 420 uC cm^{-2} is employed used to convert from the anodic CO-stripping charge to Pt ECSA. It is important to note that this value is derived based on the geometry of a Pt surface and is not accurate for other materials. Figure S7 compares CO stripping curves of experimental NCs ranging from 0.5 to 1.3 volt (vs. RHE). In general, position and areas of CO oxidation peaks at the CV curves indicate the identity (also the required voltage to drive the maximum CO oxidation kinetics) and the relative amount of surface sites that have been occupied by the CO chemisorption. As indicated for Pt-s, the CO oxidation region (0.45 V to 1.1 V vs. NHE) comprise two oxidation peaks at ca. 0.62 V (peak A) and ca. 0.83 V (peak B). Given that all experimental samples were supported at identical carbon materials, effects of interface contact and residual capacitance on the chemisorption manners can be ruled out from those CV sweeping curves. As a result, the two electro-oxidation peaks can be attributed to the CO chemisorption at surface sites with different binding energies; where the peak A and B shall relate to the sorption of CO at close packed (low sorption energy) and opened (high sorption energy) facets, respectively. A broad peak A implies the presence of multi-status CO sorption manners due to the insignificant binding energy differences between sorption sites at close-packed surfaces. The high voltage peak B refers to CO oxidation maximum in high sorption energy (opened) facets. The morphology of Pt-s NC is shown in Figure 2a and Figure S1a where distinct atomic arrangements are found in (111) and other facets (hkl, which containing high density of defects). For Pd-s NC (Figure S1c), absence of peak A in CO stripping curve royally responses the low sensitivity of CO oxidation in close packed facets of transition metal surface. The CO oxidation peaks at open facets (peak B*) is shifted to high voltage side as compared to that (peak B) of Pt-s. The broaden and split of peak B* and B- indicate the presences of varies CO sorption sites (i.e., indistinct differences of atomic arrangement as shown by HRTEM image in Figure S1c) at opened facets of Pd-s. For PdPt-p, position of peak A is substantially shifted to low energy site by 0.34 volt (peak A") and the intensity is dramatically suppressed by 90%+ as compared to those of Pt-s. Those characteristics indicate the reduced CO sorption energy and number density of sorption sites (i.e., surface Pt compositions) in close-packed facets. As consistently explained by XAS and XPS analysis, majority of Pt atoms are located in core region which passivate the close packed facet of PdPt-p. A sharp and intense current response of CO sorption (peak B") with a weak shoulder (denoted by ■) indicate the highly increased selectivity of CO

sorption in opened facets. It can be explained by the formation of unity Pt-CO bond at highly dispersed Pt atoms surrounded by Pd atoms in PdPt-p NC; where Pt atoms are mostly homogeneous distributed in NC surface. For the case of PdPt-s, slight increased (decreased) intensity of peak A" (peak B") can be explained by a higher extent of Pt exposure to NC surface as compared to those of PdPt-p. Such a rationale is consistently explained by the synthetic procedures (where Pt atoms are posited in Pd surface by sorption of Pt4+ ions in followed by a rapid reduction via interacting with strong reduction agent $NaBH_4$) and XPS analysis results (Table S1). [1] [2]

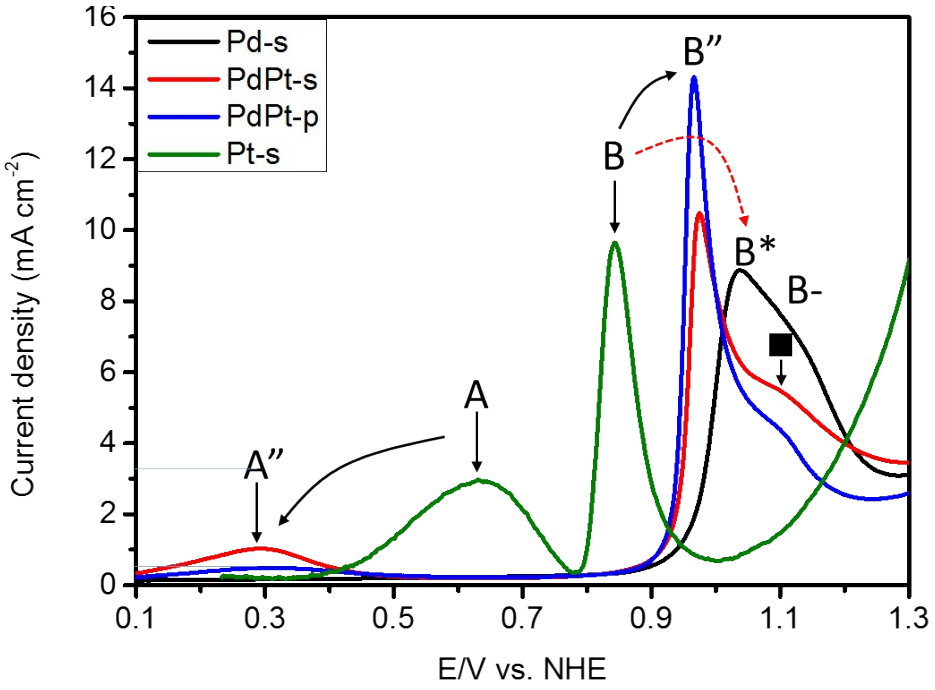

Figure S7 CO stripping curves of experimental NCs. Peak A, A", B, B*, and B- refer to current responses from oxidation of CO sorption at closed packed Pt facets, closed packed Pd facets contains certain Pt atoms, opened Pd facets with Pt atoms, close packed and opened facets of Pd crystal.

Reference

[1] R. R. Adzic, J. Zhang, K. Sasaki, M. B. Vukmirovic, M. Shao, J. X. Wang, A. U. Nilekar, M. Mavrikakis, J. A. Valerio, F. Uribe *Topics in Catalysis*. **2007**, 46, 249-262.

[2] J. Ma, A. Habrioux, C. Morais, A. Lewera, W. Vogel, Y. Verde-Gómez, G. Ramos-Sanchez, P. B. Balbuena, N. Alonso-Vante *ACS Catal.* **2013**, 3, 1940-1950.